Biodistribution of Yttrium-90–Labeled Anti-CD45 Antibody in a Nonhuman Primate Model

Eneida R. Nemecek,[1,2] Donald K. Hamlin,[5] Darrell R. Fisher,[6] Kenneth A. Krohn,[4] John M. Pagel,[1,3] Frederick R. Appelbaum,[1,3] Oliver W. Press,[1,3] and Dana C. Matthews[1,2]

[1]Division of Clinical Research, Fred Hutchinson Cancer Research Center; Departments of [2]Pediatrics, [3]Medicine, [4]Radiology, and [5]Radiation Oncology, University of Washington, Seattle, Washington; and [6]Pacific Northwest National Laboratories, Richland, Washington

ABSTRACT

Purpose: **Radioimmunotherapy may improve the outcome of hematopoietic cell transplantation for hematologic malignancies by delivering targeted radiation to hematopoietic organs while relatively sparing nontarget organs. We evaluated the organ localization of yttrium-90-labeled anti-CD45 (^{90}Y-anti-CD45) antibody in macaques, a model that had previously predicted iodine-131-labeled anti-CD45 (^{131}I-anti-CD45) antibody biodistribution in humans.**

Experimental Design: **Twelve *Macaca nemestrina* primates received anti-CD45 antibody labeled with 1 to 2 mCi of ^{90}Y followed by serial blood sampling and marrow and lymph node biopsies, and necropsy. The content of ^{90}Y per gram of tissue was determined by liquid scintillation spectrometry. Time-activity curves were constructed using average isotope concentrations in each tissue at measured time points to yield the fractional residence time and estimate radiation absorbed doses for each organ per unit of administered activity. The biodistribution of ^{90}Y-anti-CD45 antibody was then compared with that previously obtained with ^{131}I-anti-CD45 antibody in macaques.**

Results: **The spleen received 2,120, marrow 1,060, and lymph nodes 315 cGy/mCi of ^{90}Y injected. The liver and lungs were the nontarget organs receiving the highest radiation absorbed doses (440 and 285 cGy/mCi, respectively). Ytrrium-90-labeled anti-CD45 antibody delivered 2.5- and 3.7-fold more radiation to marrow than to liver and lungs, respectively. The ratios previously observed with ^{131}I-anti-CD45 antibody were 2.5-and 2.2-fold more radiation to marrow than to liver and lungs, respectively.**

Conclusions: **This study shows that ^{90}Y-anti-CD45 antibody can deliver relatively selective radiation to hematopoietic tissues, with similar ratios of radiation delivered to target versus nontarget organs, as compared with the ^{131}I immunoconjugate in the same animal model.**

INTRODUCTION

Allogeneic hematopoietic cell transplantation can cure many patients with hematologic malignancies, but relapse remains the major cause of treatment failure. Intensifying transplant preparative regimens with systemic chemotherapy and radiotherapy decreases the rate of relapse but increases the risk of transplant-related morbidity and mortality (1–4). Monoclonal antibodies reactive with hematopoietic antigens have been used as potential vehicles to deliver targeted chemotherapy or radiation therapy to sites of leukemia and lymphoma involvement (5–11). The delivery of supplemental radiation to target hematopoietic organs, with relative sparing of other nontarget organs, may decrease the risk of posttransplant relapse without excessively increasing transplant-related toxicity.

The CD45 antigen is a tyrosine phosphatase present on the surface of most nucleated hematopoietic cells, lymphoblasts, and myeloblasts, but not on the surface of nonhematopoietic cells (12, 13). This antigen is expressed in a relatively high copy number (200,000 binding sites per cell) and is not appreciably internalized after ligand binding (14, 15). Radiolabeled antibodies exert their cytotoxic effect by either directly killing antigen-positive cells to which they bind to or by killing neighboring cells within a mean path length specific for each radionuclide (16). This mechanism, known as bystander effect, poses a potential advantage when treating malignancies with heterogeneous antigen expression, such as leukemia and lymphoma, in which the antibody may not bind to every malignant cell. Given this bystander effect and the relatively high expression of CD45 antigen by normal and abnormal hematopoietic cells, a radioactive moiety attached to an anti-CD45 antibody can deliver radiation to residual leukemia cells, even in the setting of disease remission.

The ability of iodine-131-labeled anti-CD45 antibody to deliver radiation relatively selectively to hematopoietic tissues has been shown previously in mice, macaques and humans (5, 6, 17–19). Clinical studies of ^{131}I-anti-CD45 antibody combined with conventional transplant regimens have shown that this antibody can deliver at least twice as much radiation to hematopoietic organs compared with nontarget organs (5, 6). Although preliminary results of these clinical studies are encouraging, treatment still fails in many patients because of relapse or transplant-related complications, indicating the need to further improve current radioimmunotherapy methods. One approach to improve the delivery of radiation to target organs is the use of alternative radionuclides.

The β emitter, yttrium-90, has several physical properties that may result in improved ratios of radiation delivered to target compared with nontarget organs (5, 20). Unpublished preliminary studies of ^{90}Y-anti-CD45 antibody in mice done by our group showed longer retention of radionuclide in the target

Received 8/27/04; revised 10/1/04; accepted 10/26/04.
Grant support: National Cancer Institute, NIH, grants CA100394 (E. Nemecek) CA44991, (D. Matthews) and CA71077 (O. Press).
The costs of publication of this article were defrayed in part by the payment of page charges. This article must therefore be hereby marked *advertisement* in accordance with 18 U.S.C. Section 1734 solely to indicate this fact.
Requests for reprints: Eneida R. Nemecek, Fred Hutchinson Cancer Research Center, 1100 Fairview Avenue North, P. O. Box 19024, MS D5-280, Seattle, WA 98109. Phone: 206-667-1816; Fax: 206-667-5899; E-mail: enemecek@fhcrc.org.

tissues of marrow and spleen compared with ^{131}I but also longer retention of ^{90}Y in the liver. Because the relative organ concentration and retention of radiolabeled antibody may differ between mice and larger animals, we tested the hypothesis that superior delivery of radiation to target organs could be achieved with ^{90}Y in a nonhuman primate model. The biodistribution of ^{131}I-anti-CD45 antibody in previous macaque studies closely resembled the biodistribution subsequently observed for ^{131}I-anti-CD45 antibody in humans (5, 19). The macaque model also allows extensive tissue sampling and thus direct measurement of ^{90}Y in organs of interest.

In this study, we examined the relative organ localization and retention (i.e., biodistribution) of ^{90}Y-anti-CD45 antibody in macaques using direct quantitative methods and compared the results to those previously obtained with ^{131}I-anti-CD45 antibody in the same animal model.

MATERIALS AND METHODS

Animals

Twelve *Macaca nemestrina* males were obtained from and housed at the Washington National Primate Research Center of the University of Washington (Seattle, WA). The median age of the animals was 5 years (4 to 6 years), and the median weight was 7.5 kg (4.3 to 9 kg). Animal care and procedures were done in accordance to the guidelines from the Institute of Laboratory Animal Resources of the National Research Council, National Academy of Sciences, and with approval of the Institutional Animal Care and Use Committee.

Monoclonal Antibody

The monoclonal antibody AC8 is a murine IgG2a isotype that recognizes CD45 antigen of nonhuman primates, binding approximately 2×10^5 CD45 molecules per cell, with an association constant (avidity) of 5×10^8 L/mol (19, 21). Hybridoma cells secreting the AC8 antibody were provided by W. Michael Gallatin (Fred Hutchinson Cancer Research Center, Seattle, WA). Ascites was produced by inoculating the hybridoma cells into specific pathogen-free mice. The antibody was purified by batch extraction and high-performance liquid chromatography with ABx exchange resin (J.T. Baker, Phillipsburgh, NJ). The eluted antibody was pooled, concentrated, and diafiltered through a PM-10 ultrafiltration membrane (Amicon Corp, Danvers, MA) into PBS (pH 7.2; 140 mmol/L NaCl, 8 mmol/L NaH_2PO_4, 2.7 mmol/L KCl, 1.5 mmol/L KH_2PO_4). The concentration of antibody was determined using a modified bicinchoninic acid protein assay (Pierce Chemical, Rockford, IL), standardized with bovine serum albumin (Sigma, St. Louis, MO). The antibody was aliquoted and stored at −70°C until use.

Conjugation, Radiolabeling, and Characterization of the Antibody

The antibody conjugate was prepared using methods previously described (22). All reagents and laboratory ware used for conjugation and radiolabeling were metal free. Buffers were prepared with metal-free (18 Ω) water, passed over a column of Chelex 100 resin (BioRad, Hercules, CA) and sterile filtered. Plastic laboratory ware was acid washed in 1% nitric acid followed by rinsing with metal-free water. The AC8 antibody (150 mg, 15 mg/mL) was placed in a Slide-A-Lyzer 10K cassette (Pierce, Rockford, IL) and dialyzed against 4 L of saline buffer (150 mmol/L NaCl, 1 mmol/L EDTA, pH 7.0) with six buffer changes, adding 5 g of Chelex-100 resin with each buffer change, at 4°C over 3 days. The dialyzed antibody (133 mg/9.2 mL) was mixed with 9.2 mL of HEPES buffer (100 mmol/L *N*-[2-hydroxyethyl]piperazine-*N*′-ethanesulfonic acid, 150 mmol/L NaCl, and 1 mmol/L EDTA, pH 8.5) and conjugated to 5.6 mg of 1,4,7,10-tetra-azacylododecane *N*,*N*′,*N*′′,*N*′′′-tetraacetic isothiocyanate (DOTA-NCS, Macrocyclics, Dallas, TX) at room temperature for 12 hours. The antibody conjugate was then dialyzed twice against 4 L of citrate buffer (50 mmol/L Na citrate, 150 mmol/L NaCl, pH 5.5) containing 5 g of Chelex-100 resin followed by 6 × 4 L of saline (150 mmol/L NaCl, pH 7.0). The antibody was 99% pure, as confirmed by high-performance liquid chromatography and isoelectric focusing gel electrophoresis. The antibody concentration was determined to be 6 mg/mL by UV absorption at 280 nm (UV_{280}) using a DU520 spectrophotometer (Beckman Coulter, Allendale, NJ). The final product was sterile filtered and stored in metal-free vials at 4°C until use.

An aliquot of AC8-DOTA conjugate was diluted 1:1 with 0.5 mol/L ammonium acetate (pH 5.3) and 1.5 to 2 mCi of ^{90}Y-chloride (Perkin-Elmer, Boston, MA) were added. The reaction mixture was incubated at 37°C for 1 hour, passed through a PD-10 column (G-25 Sephadex, Pharmacia, Piscataway, NJ) and eluted with 0.9% saline. The protein fractions were combined and the final antibody concentration determined by UV_{280}. The radiolabeling yield was 85% to 95%. The pooled fractions of ^{90}Y-AC8 antibody were tested for immunoreactivity using a modified cell-binding assay with macaque peripheral blood lymphocytes, as previously described (23). Known amounts of antibody were diluted in RPMI 1640 (Invitrogen, Grand Island, NY) with 1% bovine serum albumin (Sigma, St. Louis, MO) and incubated with (2 to 3) × 10^5 cells for 1 hour at room temperature. Cells were washed twice after incubation, and bound radioactivity was counted. The final radiolabeled antibody product retained 75% or greater of its baseline immunoreactivity after radiolabeling and was more than 97% pure, as determined by cellulose acetate electrophoresis. The fraction of radiolabeled antibody product was combined with cold AC8 antibody to a total dose of 0.5 mg/kg antibody, diluted in PBS to a final volume of 10 mL. We chose to administer 0.5 mg/kg of AC8 antibody because the biodistribution of this non–antigen saturating dose of ^{131}I-AC8 antibody in previous macaque studies proved to be very similar to the biodistribution of 0.5 mg/kg of ^{131}I-BC8 antibody subsequently observed in humans (5, 19).

Antibody Localization Studies

Animals received a single i.v. injection of ^{90}Y-AC8 antibody over 10 minutes, under general anesthesia. They were monitored for cardiorespiratory and physical status changes during the infusion and daily until euthanasia. Blood samples were obtained before the antibody infusion, at the end of the infusion (hour 0), and 0.5, 1, 2, 24, 48, and 96 hours postinfusion to measure complete blood counts, serum chemistries, and ^{90}Y activity. Bone marrow and femoral lymph node excisional biopsies were obtained at 2 (n = 12), 24 (n = 9), 48 (n = 6), and 96 (n = 3) hours after the antibody infusion. Bone marrow core biopsies were done using a Jamshidi needle (Baxter,

Valencia, CA). After nonphysical euthanasia under sedation, necropsies were done in three animals per time point at 2, 24, 48, and 96 hours postinfusion. Triplicate core samples of approximately 100 mg were obtained from adrenal glands, bone, marrow, brain, femoral lymph nodes, gall bladder wall, heart, pancreas, kidney, lung, liver, skeletal muscle, stomach, small and large intestine wall, spleen, testis, thymus, thyroid gland, and urinary bladder wall to measure ^{90}Y tissue activity. Marrow biopsy samples obtained before the antibody infusion were evaluated by an independent pathologist for morphology and estimated to have approximately 60% cellularity, considered normal for nonhuman primates.

Blood and tissue samples were weighed, mixed with 2 mL of Solvable (Perkin-Elmer) and incubated at 56°C for 3 to 4 hours until dissolved. The ^{90}Y activity was then measured using an LS 6500 liquid scintillation spectrometer (Beckman Coulter, Allendale, NJ). After allowing 14 days for radioactivity decay, a standard solution containing 100,000 cpm of ^{90}Y was added to each sample vial and recounted for radioactivity (control samples). The ^{90}Y activity for each sample was corrected for tissue attenuation and quenching by multiplying the observed initial counts by a quotient determined by the activity in the control sample divided by the activity in an aliquot of the ^{90}Y standard solution. The quench-corrected tissue counts were compared with those of a standard aliquot of the infusion dose in each animal, and results expressed as percentage of injected dose per gram of tissue (%ID/g).

Radiation Dosimetry

Corrected tissue uptake values (%ID/g) for each time point were averaged. Time-activity curves for each source organ or tissue were then constructed and integrated to yield the fractional residence time or area under the curve, representing the average of accumulated activity in the organ divided by the administered activity (24). The residence times were applied to a dosimetry model representing the human 1-year-old (9.7 kg), and corrections were made to adjust the calculated residence times for the macaque to the appropriate dosimetry model (25). Internal radiation absorbed doses were then calculated using the method recommended by the Medical Internal Radiation Dose Committee of the Society of Nuclear Medicine (26). Radiation absorbed doses to hollow organs (i.e., intestine, gall bladder, and urinary bladder) were calculated separately because the medical internal radiation dose models assume that the activity is located in nontissue contents rather than the wall of these organs. The radiation absorbed dose for each of these organs was estimated by calculating the absorbed fraction of β energy and then multiplying that value by the equilibrium dose constant and the integral residence time per gram of tissue. Organ thickness was estimated using the models for the newborn or 1-year-old child (27). Estimates of radiation absorbed dose to marrow assumed that the biopsy samples consisted of 50% hematopoietic tissue and 50% trabecular bone or fat (24). The reported dose estimates for each organ represent a theoretical average animal because they were calculated from pooled data for each organ and time point. Single-animal dosimetry was not possible because the limited data available from serial necropsies of one animal per time point did not allow for determination of organ concentration at each time point for all the organs in each animal. However, pooled data for an average animal based on animals of similar species, age, gender, and size are highly useful for describing the most probable dosimetry in a given animal model. The dosimetry results obtained in these experiments of ^{90}Y-AC8 antibody were then compared with those obtained in a previous study of similar design using ^{131}I-AC8 at an equivalent dose in the same animal species (19).

RESULTS

Effects of ^{90}Y-AC8 Antibody Infusion

The antibody infusion was well tolerated in all animals and there were no infusion-related acute side effects. No abnormalities were observed in serum electrolytes, liver enzymes, creatinine, hematocrit, or platelet counts (data not shown). There were no significant changes in peripheral white blood cell or monocyte counts (Fig. 1). Lower lymphocyte counts ($P < 0.0001$, Kruskal-Wallis test) and increased neutrophil counts ($P = 0.027$) were observed over time. The mean (95% confidence interval) decrease in lymphocytes from the time of infusion to 96 hours postinfusion was 2175 (1130-3219) cells/mL or 55% (38-71%). The mean increase in neutrophils was 2771 (750-4792) cells/μL or 56% (35-77%).

Organ Biodistribution

Clearance of the antibody from blood was biphasic (Fig. 2). There was a short initial $t_{1/2}$ (0.4 ± 0.1 hours) and a longer β $t_{1/2}$ (14.7 ± 5.5 hours). More than 90% of the activity was cleared from blood within 24 hours after the infusion. The concentration of antibody in hematopoietic organs was higher than in nontarget organs, with spleen and marrow having the highest radiation uptake (Fig. 3). The activity at 24 hours was 2.31 ± 0.20 in spleen, 1.63 ± 0.21 in marrow, and 0.40 ± 0.04 %ID/g in lymph nodes. The highest uptake in spleen was observed immediately after the antibody infusion, likely reflecting the rapid blood pooling in this organ. Marrow and lymph nodes had their highest uptake approximately 24 hours after the antibody infusion. The nontarget organ with the highest radiation uptake was the liver followed by lungs and kidney. The highest activity in nontarget organs was observed immediately after the antibody infusion. The activity at 24 hours was 0.33 ± 0.05 in liver, 0.27 ± 0.03 in lungs, and 0.13 ± 0.02 %ID/g in kidneys. The radiation uptake for other nontarget organs was negligible, never exceeding 0.05 %ID/g (data not shown). Retention of activity in nontarget organs was minimal after 48 hours.

Similarly, our previous studies with ^{131}I-AC8 showed blood clearance to be biphasic, with an initial $t_{1/2}$ of 0.6 ± 0.1 hours and a β $t_{1/2}$ of 56.5 ± 25.4 hours (Fig. 2; ref. 19). The activity at 24 hours was 0.78 ± 0.02 in spleen, 0.11 ± 0.05 in marrow, 0.12 ± 0.03 in lymph nodes, 0.07 ± 0.02 in liver, 0.06 ± 0.04 in lungs, and 0.01 ± 0.001 %ID/g in kidneys (Fig. 3). All target and nontarget organs had their highest radiation uptake immediately after the antibody infusion. The nontarget organs having the highest radiation uptake were liver and lungs. Compared to ^{131}I-AC8 antibody, ^{90}Y-AC8 antibody resulted in higher activity in marrow, liver, lungs, and kidneys for the first 24 hours and in similar activity after 48 hours.

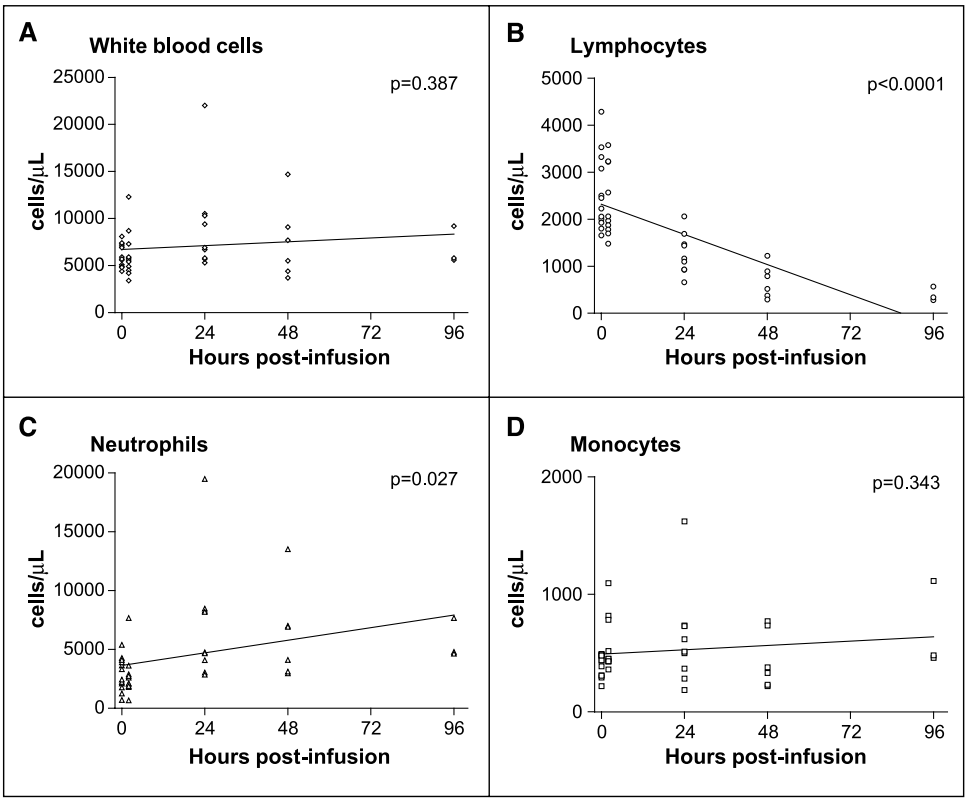

Fig. 1 Peripheral white blood cell, lymphocyte, neutrophil, and monocyte counts after infusion of ^{90}Y-AC8 antibody in macaques.

Estimated Radiation Absorbed Doses

The estimated radiation absorbed doses were higher for bone marrow and spleen than for nontarget organs (Table 1). The liver was the nontarget organ receiving the highest radiation dose. The ^{90}Y-AC8 antibody delivered 4.8 times greater radiation to the spleen and 2.5 times greater radiation to the marrow than to the liver. The dose to lymph nodes was 28% lower than the dose to liver. The dose to spleen was 7.4 times greater and the dose to marrow was 3.7 times greater than that to the lungs, the nontarget organ receiving the second highest radiation dose.

Table 2 summarizes the ratio of estimated radiation absorbed doses to target versus nontarget organs (i.e., therapeutic ratio) achieved with ^{90}Y- or ^{131}I-labeled AC8 antibody for an average animal. Both radioimmunoconjugates delivered higher doses of radiation to spleen and marrow than to nontarget organs. Compared to ^{131}I-labeled antibody, ^{90}Y-labeled antibody resulted in a higher ratio (168%) of marrow to lung, and in lower ratios of lymph node to liver (30%) and spleen to liver (50%). All other ratios were similar for both radioimmunoconjugates.

DISCUSSION

This study shows the ability of ^{90}Y-labeled anti-CD45 antibody to deliver relatively targeted radiation to hematopoietic tissues. The marrow to nontarget organ ratio of radiation observed with ^{90}Y-labeled anti-CD45 antibody is similar to that achieved with the ^{131}I-labeled antibody.

In previous macaque experiments, we evaluated the biodistribution and dosimetry of two ^{131}I-labeled antibodies reactive with the CD45 antigen of nonhuman primates (19). The animals received either 0.5 mg/kg of ^{131}I-BC8, an antibody reactive with human CD45 with moderate avidity and nonhuman primate CD45 with low avidity, or 0.5 mg/kg (low dose) or 4.5 mg/kg (high dose) of ^{131}I-AC8 antibody, an antibody reactive with nonhuman primate CD45 with moderate avidity. Organ residence times for ^{131}I were generated from serial quantitative γ images and direct measurement of ^{131}I concentration in tissue samples. The extent and pattern of antibody bound to target cells was

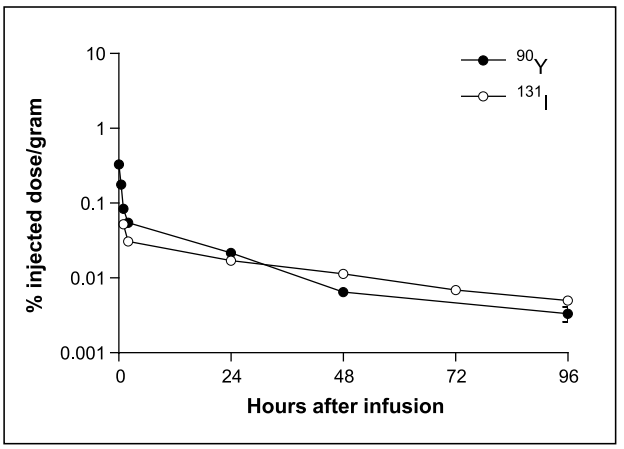

Fig. 2 Clearance of ^{90}Y-AC8 and ^{131}I-AC8 antibody from blood. Percent of injected dose per gram of blood (mean ± SE) in a logarithmic scale.

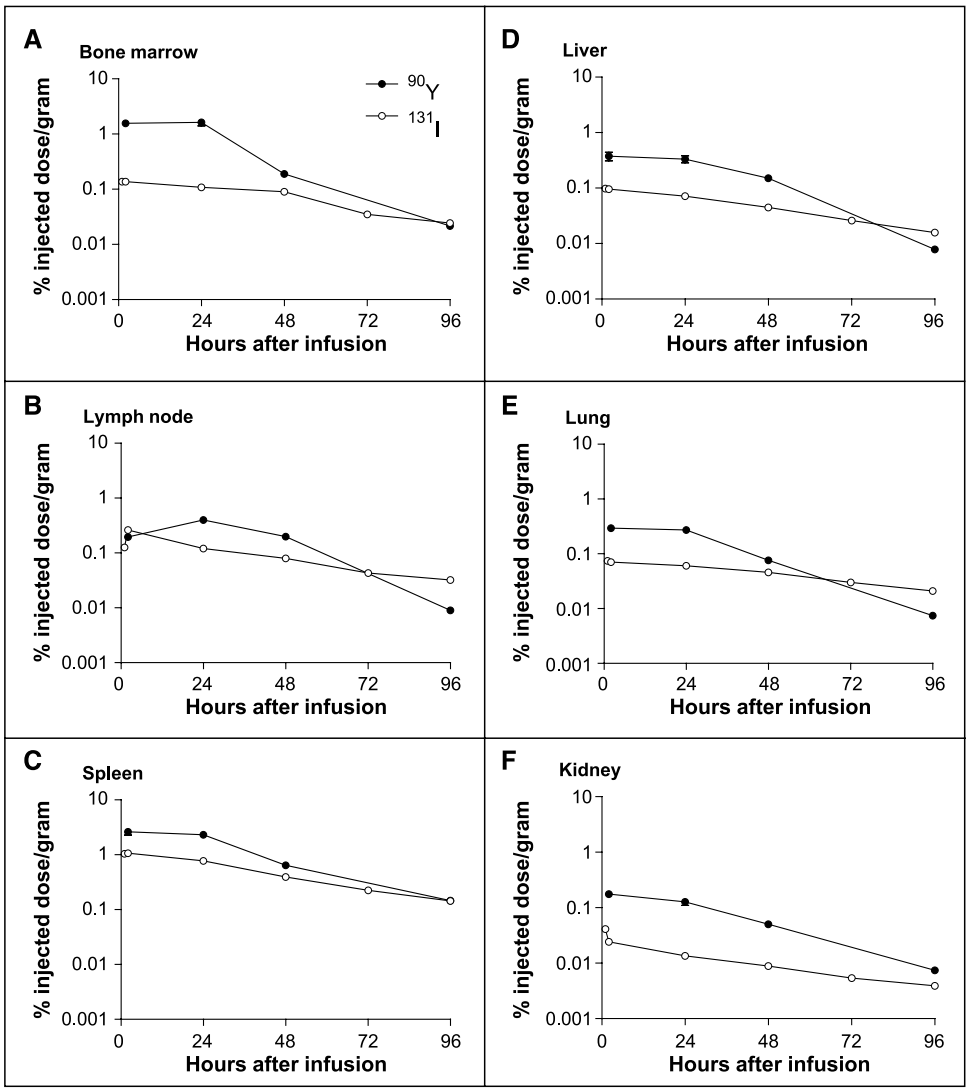

Fig. 3 Clearance of ^{90}Y-AC8 and ^{131}I-AC8 antibody from target and nontarget organs. Percent of injected dose per gram of tissue (mean ± SE) in a logarithmic scale.

measured by flow microfluometry. Low-dose BC8 cleared more slowly from blood and had a higher and more homogeneous uptake in lymph nodes than low-dose AC8. High-dose AC8 saturated all CD45 antigen sites on node lymphocytes. This difference in binding to antigenic sites was thought to be related to differences in avidity between the two antibodies, although an effect of different isotypes could not be excluded. The nontarget organs with the highest radiation uptake were lungs and liver. Low-dose ^{131}I-AC8 antibody delivered estimated radiation absorbed doses 8 to 9 times higher to spleen, 2 to 3 times higher to marrow, and 2 times higher to lymph nodes than to lungs or liver.

In our study, ^{90}Y-AC8 antibody delivered estimated radiation absorbed doses 5 to 7 times higher to spleen and 2 to 4 times higher to marrow than to lungs or liver. The estimated radiation absorbed dose to lymph nodes was 28% lower than the dose to liver and 10% higher than the dose to lungs. The high avidity of AC8 for macaque CD45 antigen may result in more rapid uptake by cells in tissues readily accessible to the circulation such as spleen and bone marrow than in lymph nodes (19). At the same antibody dose, the radiation delivered to lymph nodes with ^{131}I was higher than that achieved with ^{90}Y. We have observed similar results in limited, unpublished studies of ^{90}Y-anti-CD45 antibody in mice. The reason for this finding is unclear, but it could be explained in part by differences in uptake and biological retention times in lymph nodes, or differences in physical half-life between both isotopes. Preliminary studies labeling anti-CD45 antibody with bismuth-213, an α emitter of shorter half-life, very high energy, and much shorter path length than ^{131}I or ^{90}Y have yielded similar results (28, 29).

Iodine-131 isotope was initially selected as the radiolabel for our clinical studies given its low cost, ready availability, long track record in the clinical setting, simple chemistry for radiolabeling, and capacity for imaging by using conventional planar nuclear scanning. Although these preclinical studies with directly labeled ^{90}Y-AC8 antibody do not show a therapeutic advantage for ^{90}Y compared with ^{131}I, there are several reasons

to consider this radiometal immunoconjugate for future clinical use. First, its shorter physical half-life of 2.7 days matches the biological half-life of anti-CD45 antibody more closely than the 8-day physical half-life of ^{131}I (5). In addition, the higher β-particle energy and resulting longer path length of ^{90}Y could improve the homogeneity of radiation delivered to target tissues, particularly in the complex marrow environment in which trabecular bone may prevent penetration of the lower β-particle energy of ^{131}I (20, 30, 31). There are also practical advantages to the use of ^{90}Y in the clinical setting. A large number of patients treated in our clinical trials with anti-CD45 antibody labeled with high doses of ^{131}I have developed hypothyroidism secondary to radioablation despite use of prophylactic thyroid blockade with iodine p.o. solution (5). This toxicity can be avoided by using ^{90}Y, as shown by the low uptake of this gland on the macaque dosimetry model. Contrary to ^{131}I, ^{90}Y does not produce γ emissions and does not require confinement of patients in radiation isolation rooms, a significant advantage in terms of health personnel safety and ease of treatment in the outpatient setting (32).

However, the lack of γ emissions of ^{90}Y also limits the utility of conventional planar nuclear imaging for direct determination of the concentration of this radionuclide in organs of interest. Because the standard method for evaluating the biodistribution of a radiolabeled antibody is to measure the concentration of radioactivity uptake within each organ, several alternative imaging techniques for ^{90}Y are being explored. The first and most studied technique involves γ imaging using indium-111 as a surrogate isotope (33–35). The second involves measuring ^{90}Y bremsstrahlung radiation (36–38). Positron emission tomography with the less readily available radionuclide yttrium-86 has also been studied and may potentially yield more accurate dosimetry results than ^{111}In or bremsstrahlung imaging (39, 40). These techniques have been evaluated in studies of lymphoma, breast, hepatic, and gastrointestinal malignancies (38–43). There are no preclinical or clinical studies to date comparing the accuracy of these imaging methods.

Table 1 Organ dosimetry of ^{90}Y-AC8 antibody for a theoretical average animal

Organ	cGy/mCi*
Target organs	
Spleen	2,120
Bone marrow	1,060
Lymph nodes	315
Nontarget organs	
Liver	440
Lungs	285
Kidneys	136
Adrenal glands	108
Cortical bone	89.2
Heart wall	39.5
Testes	35.3
Thymus	30.1
Muscle	30
Pancreas	25.2
Thyroid gland	25.1
Stomach	24.8
Gallbladder wall	17.1
Urinary bladder	12.8
Small intestines	12.4
Whole body	11.9
Colon	11.3
Brain	3.3
Skin	1.3

*Estimated radiation absorbed doses per millicurie of ^{90}Y injected.

Table 2 Comparison of therapeutic ratios for ^{90}Y- and ^{131}I-AC8 antibody

Ratio*	^{90}Y-AC8	^{131}I-AC8
Spleen:liver	4.8	9.1
Marrow:liver	2.5	2.5
Lymph nodes:liver	0.7	2.0
Spleen:lungs	7.4	7.9
Marrow:lungs	3.7	2.2
Lymph nodes:lungs	1.1	1.7

*Results represent the average target-to-nontarget organ ratio of radiation after injection of 0.5 mg/kg of antibody labeled with ^{90}Y (n = 12) or ^{131}I (n = 3; ref. 19).

Regardless of the radionuclide used, residual unbound radiolabeled antibody in the circulation and the resultant high levels of background radioactivity are obstacles to the optimal implementation of radioimmunotherapy, limiting the target to nontarget organ ratios of absorbed radiation that can be achieved. New radioimmunotherapy techniques are focusing on reducing the amount of unbound radiolabeled antibody from the circulation in an attempt to reduce toxicity to nontarget organs. One attractive approach, pretargeting, consists of a multistep process to dissociate the distribution phase of the antibody protein from the administration of the therapeutic radionuclide (44-48). A second approach is the removal of antibody from the circulation using extracorporeal adsorption therapy (49). We have initiated studies testing these approaches with anti-CD45 in a nonhuman primate model, with the goal to improve the ratios of radiation to target versus nontarget organs observed in the study described here.

Our study confirms that radiolabeled antibody reactive against CD45 antigen can deliver significantly greater radiation to target organs compared with nontarget organs. Labeling this antibody with ^{90}Y resulted in therapeutic ratios similar to those observed previously with ^{131}I. However, this comparison was limited by several factors. First, there were differences in the methods to obtain radiation absorbed dose estimates in the macaques treated with ^{131}I or ^{90}Y. For the initial studies with ^{131}I the data were obtained from both γ imaging (indirect) and direct quantification of tissue radioactivity, which allowed for determination of dosimetry for each individual animal. For the ^{90}Y studies, only direct quantification methods were used, thus not allowing determination of dosimetry for each animal but rather for an average animal. We attempted to compensate for this lack of imaging data by studying the largest number of animals per time point possible. However, our ability to study an even larger number of animals was limited by the financial and ethical constraints of research with primates. Despite these limitations, this study provides important information about the feasibility of ^{90}Y-labeled anti-CD45 antibody therapy and extensive quantitative data of the biodistribution of this radioimmunoconjugate in a nonhuman primate model, both of utility for the design of future clinical trials.

ACKNOWLEDGMENTS

We thank the veterinary and research staff of the Washington National Primate Research Center for their technical support; the Radiation Safety officers of the University of Washington and Fred Hutchinson Cancer Research Center; Cyd Nourigat and the Pediatric Oncology laboratory technicians for providing the BC8 antibody; Dr. Robert Andrews and Jennifer C. Potter for their assistance with immunoreactivity assays; Dr. David Myerson for performing the marrow pathology studies; Dr. Brenda Sandmaier for providing the liquid scintillation spectrometer; Dr. D. Scott Wilbur for providing his radiolabeling expertise; and Lawrence Durack and Dr. Janet Eary for assistance with nuclear medicine and radiation regulatory issues.

REFERENCES

1. Bearman SI, Appelbaum FR, Buckner CD, et al. Regimen-related toxicity in patients undergoing bone marrow transplantation. J Clin Oncol 1988;6:1562–8.

2. Clift RA, Buckner CD, Appelbaum FR, et al. Allogeneic marrow transplantation in patients with acute myeloid leukemia in first remission: a randomized trial of two irradiation regimens. Blood 1990;76:1867–71.

3. Demirer T, Petersen FB, Appelbaum FR, et al. Allogeneic marrow transplantation following cyclophosphamide and escalating doses of hyperfractionated total body irradiation in patients with advanced lymphoid malignancies: a phase I/II trial. Int J Radiat Oncol Biol Phys 1995;32:1103–9.

4. Demirer T, Buckner CD, Appelbaum FR, et al. Busulfan, cyclophosphamide and fractionated total body irradiation for autologous or syngeneic marrow transplantation for acute and chronic myelogenous leukemia: phase I dose escalation of busulfan based on targeted plasma levels. Bone Marrow Transplant 1996;17:491–5.

5. Matthews DC, Appelbaum FR, Eary JF, et al. Phase I study of (131)I-anti-CD45 antibody plus cyclophosphamide and total body irradiation for advanced acute leukemia and myelodysplastic syndrome. Blood 1999;94:1237–47.

6. Ruffner KL, Matthews DC. Current uses of monoclonal antibodies in the treatment of acute leukemia. Semin Oncol 2000;27:531–9.

7. Sievers EL, Larson RA, Stadtmauer EA, et al. Efficacy and safety of gemtuzumab ozogamicin in patients with CD33-positive acute myeloid leukemia in first relapse. J Clin Oncol 2001;19:3244–54.

8. Bunjes D, Buchmann I, Duncker C, et al. Rhenium 188-labeled anti-CD66 (a, b, c, e) monoclonal antibody to intensify the conditioning regimen prior to stem cell transplantation for patients with high-risk acute myeloid leukemia or myelodysplastic syndrome: results of a phase I-II study. Blood 2001;98:565–72.

9. Witzig TE, Gordon LI, Cabanillas F, et al. Randomized controlled trial of yttrium-90-labeled ibritumomab tiuxetan radioimmunotherapy versus rituximab immunotherapy for patients with relapsed or refractory low-grade, follicular, or transformed B-cell non-Hodgkin's lymphoma. J Clin Oncol 2002;20:2453–63.

10. Burke JM, Caron PC, Papadopoulos EB, et al. Cytoreduction with iodine-131-anti-CD33 antibodies before bone marrow transplantation for advanced myeloid leukemias. Bone Marrow Transplant 2003;32:549–56.

11. Gopal AK, Gooley TA, Maloney DG, et al. High-dose radioimmunotherapy versus conventional high-dose therapy and autologous hematopoietic stem cell transplantation for relapsed follicular non-Hodgkin lymphoma: a multivariable cohort analysis. Blood 2003; 102:2351–7.

12. Omary MB, Trowbridge IS, Battifora HA. Human homologue of murine T200 glycoprotein. J Exp Med 1980;152:842–52.

13. Andres TL, Kadin ME. Immunologic markers in the differential diagnosis of small round cell tumors from lymphocytic lymphoma and leukemia. Am J Clin Pathol 1983;79:546–52.

14. van der Jagt RH, Badger CC, Appelbaum FR, et al. Localization of radiolabeled antimyeloid antibodies in a human acute leukemia xenograft tumor model. Cancer Res 1992;52:89–94.

15. Press OW, Howell-Clark J, Anderson S, Bernstein I. Retention of B-cell-specific monoclonal antibodies by human lymphoma cells. Blood 1994;83:1390–7.

16. Nourigat C, Badger CC, Bernstein ID. Treatment of lymphoma with radiolabeled antibody: elimination of tumor cells lacking target antigen. J Natl Cancer Inst 1990;82:47–50.

17. Matthews DC, Badger CC, Fisher DR, et al. Selective radiation of hematolymphoid tissue delivered by anti-CD45 antibody. Cancer Res 1992;52:1228–34.

18. Matthews DC, Martin PJ, Nourigat C, Appelbaum FR, Fisher DR, Bernstein ID. Marrow ablative and immunosuppressive effects of 131I-anti-CD45 antibody in congenic and H2-mismatched murine transplant models. Blood 1999;93:737–45.

19. Matthews DC, Appelbaum FR, Eary JF, et al. Radiolabeled anti-CD45 monoclonal antibodies target lymphohematopoietic tissue in the macaque. Blood 1991;78:1864–74.

20. Press OW, Shan D, Howell-Clark J, et al. Comparative metabolism and retention of iodine-125, yttrium-90, and indium-111 radioimmunoconjugates by cancer cells. Cancer Res 1996;56:2123–9.

21. Gallatin WM, Wayner EA, Hoffman PA, St John T, Butcher EC, Carter WG. Structural homology between lymphocyte receptors for high endothelium and class III extracellular matrix receptor. Proc Natl Acad Sci U S A 1989;86:4654–8.

22. Mirzadeh S, Brechbiel MW, Atcher RW, Gansow OA. Radiometal labeling of immunoproteins: covalent linkage of 2-(4-isothiocyanatobenzyl)diethylenetriaminepentaacetic acid ligands to immunoglobulin. Bioconjug Chem 1990;1:59–65.

23. Badger CC, Krohn KA, Bernstein ID. *In vitro* measurement of avidity of radioiodinated antibodies. Int J Radiat Appl Instrum B 1987;14:605–10.

24. Fisher DR, Badger CC, Breitz H, et al. Internal radiation dosimetry for clinical testing of radiolabeled monoclonal antibodies. Antibody Immunoconjug Radiopharm 1991;4:655–64.

25. Cristy M, Eckerman KF. Specific absorbed fractions of energy at various ages from internal photon sources, ORNL/TM-8381, v. 1-7. Oak Ridge (TN): Oak Ridge National Laboratory; 1987.

26. Stabin MG. MIRDOSE: personal computer software for internal dose assessment in nuclear medicine. J Nucl Med 1996;37:538–46.

27. Snyder WS, Cook MJ, Nasset ES, Karhausen LR, Howells GP, Tipton IH. Report of the task group on reference man. International Commission on Radiological Protection, ICRP Report No. 23. Oxford (England): Pergamon Press; 1975.

28. Sandmaier BM, Bethge WA, Wilbur DS, et al. Bismuth 213-labeled anti-CD45 radioimmunoconjugate to condition dogs for nonmyeloablative allogeneic marrow grafts. Blood 2002;100:318–26.

29. Bethge WA, Wilbur DS, Storb R, et al. Selective T-cell ablation with bismuth-213-labeled anti-TCR TCRαβ as nonmyeloablative conditioning for allogeneic canine marrow transplantation. Blood 2003; 101:5068–75.

30. Nemecek ER, Matthews DC. Antibody-based therapy of human leukemia. Curr Opin Hematol 2002;9:316–21.

31. Fritzberg AR, Berninger RW, Hadley SW, Wester DW. Approaches to radiolabeling of antibodies for diagnosis and therapy of cancer. Pharm Res 1988;5:325–34.

32. Leonard JP, Siegel JA, Goldsmith SJ. Comparative physical and pharmacologic characteristics of iodine-131 and yttrium-90: implications for radioimmunotherapy for patients with non-Hodgkin's lymphoma. Cancer Invest 2003;21:241–52.

33. Leichner PK, Akabani G, Colcher D, et al. Patient-specific dosimetry of indium-111- and yttrium-90-labeled monoclonal antibody CC49. J Nucl Med 1997;38:512–6.

34. DeNardo SJ, Richman CM, Goldstein DS, et al. Yttrium-90/indium-111-DOTA-peptide-chimeric L6: pharmacokinetics, dosimetry and initial results in patients with incurable breast cancer. Anticancer Res 1997; 17:1735–44.

35. Cremonesi M, Ferrari M, Zoboli S, et al. Biokinetics and dosimetry in patients administered with (111)In-DOTA-Tyr(3)-octreotide:

implications for internal radiotherapy with (90)Y-DOTATOC. Eur J Nucl Med 1999;26:877–86.

36. Dillehay LE, Mayer R, Zhang YG, et al. Use of bremsstrahlung radiation to monitor Y-90 tumor and whole body activities during experimental radioimmunotherapy in mice. Cancer 1994;73:945–50.

37. Shen S, DeNardo GL, Yuan A, DeNardo DA, DeNardo SJ. Planar γ camera imaging and quantitation of yttrium-90 bremsstrahlung. J Nucl Med 1994;35:1381–9.

38. Sarfaraz M, Kennedy AS, Cao ZJ, et al. Physical aspects of yttrium-90 microsphere therapy for nonresectable hepatic tumors. Med Phys 2003;30:199–203.

39. Rosch F, Herzog H, Plag C, et al. Radiation doses of yttrium-90 citrate and yttrium-90 EDTMP as determined via analogous yttrium-86 complexes and positron emission tomography. Eur J Nucl Med 1996; 23:958–66.

40. Jamar F, Barone R, Mathieu I, et al. 86Y-DOTA(0)-D-Phe1-Tyr3-octreotide (SMT487)—a phase 1 clinical study: pharmacokinetics, biodistribution and renal protective effect of different regimens of amino acid co-infusion. Eur J Nucl Med Mol Imaging 2003; 30:510–8.

41. Vriesendorp HM, Herpst JM, Germack MA, et al. Phase I-II studies of yttrium-labeled antiferritin treatment for end-stage Hodgkin's disease, including Radiation Therapy Oncology Group 87-01. J Clin Oncol 1991; 9:918–28.

42. Wiseman GA, White CA, Stabin M, et al. Phase I/II ^{90}Y-Zevalin (yttrium-90 ibritumomab tiuxetan, IDEC-Y2B8) radioimmunotherapy dosimetry results in relapsed or refractory non-Hodgkin's lymphoma. Eur J Nucl Med 2000;27:766–77.

43. Wong JY, Somlo G, Odom-Maryon T, et al. Initial clinical experience evaluating yttrium-90-chimeric T84.66 anticarcinoembryonic antigen antibody and autologous hematopoietic stem cell support in patients with carcinoembryonic antigen-producing metastatic breast cancer. Clin Cancer Res 1999;5:3224s–31s.

44. Knox SJ, Goris ML, Tempero M, et al. Phase II trial of yttrium-90-DOTA-biotin pretargeted by NR-LU-10 antibody/streptavidin in patients with metastatic colon cancer. Clin Cancer Res 2000;6:406–14.

45. Cremonesi M, Ferrari M, Chinol M, et al. Three-step radioimmunotherapy with yttrium-90 biotin: dosimetry and pharmacokinetics in cancer patients. Eur J Nucl Med 1999;26:110–20.

46. Axworthy DB, Reno JM, Hylarides MD, et al. Cure of human carcinoma xenografts by a single dose of pretargeted yttrium-90 with negligible toxicity. Proc Natl Acad Sci U S A 2000;97:1802–7.

47. Zhang M, Yao Z, Garmestani K, et al. Pretargeting radioimmunotherapy of a murine model of adult T-cell leukemia with the α-emitting radionuclide, bismuth 213. Blood 2002;100:208–16.

48. Pagel JM, Hedin N, Subbiah K, et al. Comparison of anti-CD20 and anti-CD45 antibodies for conventional and pretargeted radioimmunotherapy of B-cell lymphomas. Blood 2003;101:2340–8.

49. Linden O, Kurkus J, Garkavij M, et al. A novel platform for radioimmunotherapy. Extracorporeal depletion of biotinylated and ^{90}Y-labeled anti-CD20 in patients with refractory B-cell lymphoma [abstract]. J Clin Oncol 2004;22:6576.

Clinical Cancer Research

Biodistribution of Yttrium-90–Labeled Anti-CD45 Antibody in a Nonhuman Primate Model

Eneida R. Nemecek, Donald K. Hamlin, Darrell R. Fisher, et al.

Clin Cancer Res 2005;11:787-794.